Avalanche Photodiode Arrays for Optical Communications Receivers

M. Srinivasan[1] and V. Vilnrotter[1]

An avalanche photodiode (APD) array for ground-based optical communications receivers is investigated for the reception of optical signals through the turbulent atmosphere. Kolmogorov phase screen simulations are used to generate realistic spatial distributions of the received optical field. It is shown that use of an APD array for pulse-position modulation detection can improve performance by up to 4 dB over single APD detection in the presence of turbulence, but that photon-counting detector arrays yield even greater gains.

I. Introduction

Ground-based reception of optical signals from space suffers from degradation of the optical phase front caused by atmospheric turbulence, leading to a reduction in the effective diameter of the receiving telescope and to random fluctuations of the point-spread function in the focal plane. A proportional increase in the receiver's field of view in order to collect all of the signal also causes a corresponding increase in the amount of interfering background radiation, resulting in degraded communications performance. These problems may be mitigated through the use of an optical detector array assembly in the focal plane that can adaptively select areas of higher signal density while ignoring areas predominated by background noise. In [1], the performance of a detector array composed of photon-counting detectors was evaluated and found to yield up to a 5 dB improvement over a conventional single-detector photon-counting receiver. However, the current baseline receiver design for deep-space optical communication utilizes readily available avalanche photodiode detectors (APDs) rather than photon-counting detector arrays, which are still in the development stage at the wavelengths of interest for optical communications. In this article, we extend some of the results obtained in [1] to the APD array case.

II. APD Output Model

In [1], the derivations of signal models for the single photon counter and the photon-counting array were given in considerable detail in order to obtain the optimally weighted photon-counting array performance. It was then shown that a suboptimal array (referred to as the adaptive synthesized detector or 0-1 subarray) consisting of the optimal number of unweighted array elements (i.e., weights of zero or one) yielded performance very near to that of the optimally weighted array. In this article, we present results

[1] Communications Systems and Research Section.

The research described in this publication was carried out by the Jet Propulsion Laboratory, California Institute of Technology, under a contract with the National Aeronautics and Space Administration.

for the 0-1 APD subarray. In our discussion of APD output statistic modeling, we follow the formulation found in [2].

The average number of photons absorbed by an APD illuminated with total optical intensity $\lambda(t)$ in T_s seconds can be expressed as

$$\bar{n} = \frac{\eta}{h\nu} \int_0^{T_s} \lambda(t) dt \tag{1}$$

where h is Planck's constant, ν is the optical frequency, and η is the detector's quantum efficiency, defined as the ratio of absorbed to incident photons. The actual number of photons absorbed, n, is a Poisson-distributed random variable with probability

$$p(n|\bar{n}) = \frac{\bar{n}^n}{n!} e^{-\bar{n}} \tag{2}$$

The probability $p(m|\bar{n})$ that an APD generates m output electrons given $\bar{n}$ mean absorbed photons can be derived from the McIntyre–Conradi distribution [3], but may be approximated by the continuous Webb density function [4] or by a Gaussian density [2,5]. Added to the random number of APD output electrons is an independent Gaussian thermal noise charge from the follow-on electronics [2]. For M-ary pulse-position modulation (PPM) with slot duration T_s, the total charge is integrated over each slot time, T_s, resulting in a vector of M independent observables for each received PPM word. It was shown in [6] that, given these observables, the maximum-likelihood detector structure consists of choosing the PPM symbol corresponding to the slot with the largest accumulated charge value.

In this article, we use the Gaussian approximation for $p(m|\bar{n})$ in order to simplify calculation of PPM symbol-error probabilities. This approximation is adequate for high background conditions, as shown in [5]. The slot statistic consisting of the sum of APD output electrons and amplifier thermal noise is thus also Gaussian, leading to M-ary PPM symbol-error probability given by

$$P_M(E) = \int_{-\infty}^{\infty} \phi\left(x, \mu_s, \sigma_s^2\right) \left[1 - \Phi\left(\frac{x - \mu_b}{\sigma_b}\right)^{M-1}\right] dx \tag{3}$$

where $\phi(x, \mu, \sigma^2)$ is the Gaussian density function with mean μ and variance σ^2, and $\Phi(x)$ is the Gaussian distribution function. The background and signal means and variances are given by $\mu_b = qG\bar{n}_b + I_s T_s$, $\mu_s = qG(\bar{n}_b + \bar{n}_s) + I_s T_s$, $\sigma_b^2 = \left[2q^2G^2F\bar{n}_b + 2qI_sT_s + (4\kappa T T_s/R_L)\right] BT_s$, and $\sigma_s^2 = \left[2q^2G^2F(\bar{n}_b + \bar{n}_s) + 2qI_sT_s + (4\kappa T T_s/R)\right] BT_s$ [2]. Here, $F = kG + (2 - 1/G)(1 - k)$, G is the average APD gain, k is the APD ionization ratio, q is the electron charge, κ is Boltzmann's constant, T is the equivalent noise temperature, B is the single-sided noise bandwidth, R is the load resistance, and I_s is the APD surface-leakage current. The mean numbers of absorbed background and signal photons are given by $\bar{n}_b$ and $\bar{n}_s$, respectively. The noise bandwidth, B, is set to that of an ideal T_s second integrator, i.e., $B = 1/2T_s$. The APD bulk dark current is modeled as part of the background radiation, i.e., it is incorporated into the value of $\bar{n}_b$.

III. Adaptive Synthesized Array

If we consider a rectangular array of detectors consisting of $K \times L$ detector elements, the optical signal intensity incident upon each array element may be denoted by $\lambda_{ij}(t)$, where $1 \le i \le K$ and $1 \le j \le L$. The average number of photons incident upon the ijth detector is then $\bar{n}_{ij} = (\eta/h\nu) \int_0^{T_s} \lambda_{ij}(t) dt$. Using

the APD modeling described above and assuming that each array element observes the sum of a signal field plus multimode Gaussian noise field with an average noise count per mode much less than one, the outputs of the APD array may be modeled as conditionally independent Gaussian processes, conditioned on the average signal intensity over each detector element [7,8]. Given the APD array-element observables, the optimum maximum-likelihood detection scheme may be derived, consisting of a weighted sum of array outputs [1]. We consider a simpler real-time suboptimum detector whose array weights are either zero or one, i.e., the array-element outputs are either included or excluded at any given time in making a PPM symbol decision. We therefore list the detector elements in decreasing order of average signal intensity, $\bar{n}_{ij}$, and compute the probability of error for the first detector element's signal intensity plus the background incident upon that element, then form the sum of signal energies from the first two detector elements (plus background for two detector elements), and so on, until the minimum error probability is reached. Each set of detectors may be effectively considered to be a single detector, so that no weighting is applied to account for variations in the signal distribution over the detector elements included in that set. The set of detector elements that achieves the minimum probability of error is the best "synthesized single detector" matched to the signal-intensity distribution. As in [1], a sample signal-intensity distribution may be generated using Kolmogorov phase-screen algorithms [9]. Note also that the process of optimizing the subarray requires calculation of the PPM symbol-error probability for each number of detectors, as well as knowledge of signal and background energy levels. A practical real-time implementation of this array detection scheme will involve additional parameter-estimation algorithms that have yet to be developed.

In evaluating the performance of an APD array, we must use an appropriate model for the thermal-noise contribution due to follow-on electronics in order to arrive at appropriate values for the load resistance, R, constrained by maintaining sufficient bandwidth to reproduce the signal pulse. We make the following assumption: the detector elements are followed by individual transimpedance amplifiers, each of which has a feedback resistance whose value is determined by $R = 7 \times 10^{12} T_s$ ohms, as per the FOCAS optical link budget program [10]. The outputs of these amplifiers may then be sampled and added together digitally to obtain the desired signal, as illustrated in Fig. 1. With fine enough quantization, the sampling and summing operations may be considered to be essentially noiseless for this application. Note that the total variance due to thermal noise at the output is the sum of the individual thermal-noise variance contributions from the load (i.e., feedback) resistors following each of the detectors.

Assuming the above model, the charge accumulated during each time slot for the ijth detector element is Gaussian distributed with mean $\mu_{ij} = qG\bar{n}_{ij} + I_s T_s$ and variance $\sigma_{ij}^2 = q^2 GF\bar{n}_{ij} + qI_s T_s + 2\kappa T T_s / R_j$, where $\bar{n}_{ij}$ is given by $\bar{n}_{s,ij} + \bar{n}_b$ for a signal slot and $\bar{n}_b$ for a noise slot. Since the outputs from the detector elements are independent Gaussian random variables, the composite signal from adding N detector outputs belonging to subset $\mathcal{S}$ has mean

$$\sum_{i,j \in \mathcal{S}} \mu_{ij} = \begin{cases} qG \sum_{i,j \in \mathcal{S}} \bar{n}_{s,ij} + NI_s T_s + NqG\bar{n}_b & \text{signal slot} \\ NqG\bar{n}_b + NI_s T_s & \text{noise slot} \end{cases} \tag{4}$$

and variance

$$\sum_{i,j \in \mathcal{S}} \sigma_{ij}^2 = \begin{cases} q^2 GF \sum_{i,j \in \mathcal{S}} \bar{n}_{s,ij} + NqI_s T_s + \dfrac{2N\kappa T T_s}{R} & \text{signal slot} \\ NqI_s T_s + \dfrac{2N\kappa T T_s}{R} & \text{noise slot} \end{cases} \tag{5}$$

where $\mathcal{S}$ denotes the set of detector elements selected for best performance, and where we have assumed that each transimpedance amplifier has the same feedback resistance value of $R = 218,750$ ohms as determined from FOCAS for the required signal bandwidth of 32 MHz. Therefore, as the number of

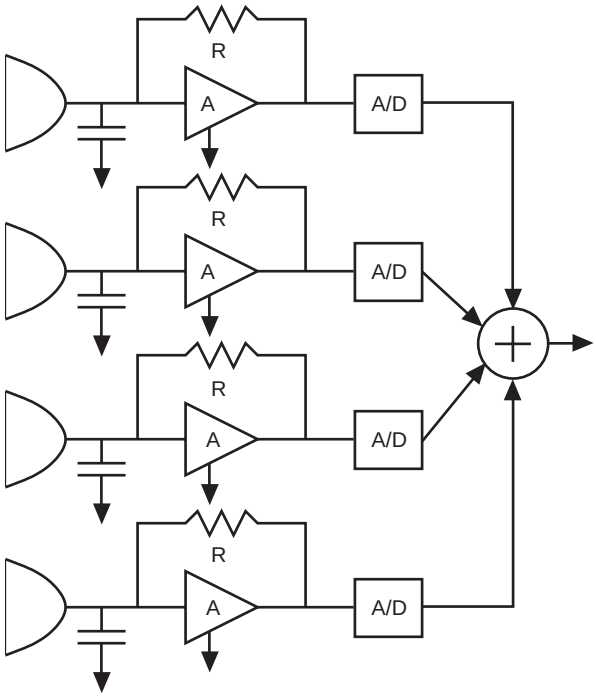

Fig. 1. Load resistance models for an APD array (where resistors are denoted by "R," amplifiers by "A," and analog-to-digital converters by "A/D").

detectors, N, in the subarray increases, the effective total load resistance used for computing the variance of the combined output varies as R/N. The other parameters used in the calculations were $G = 100$, $k = 0.07$, $T = 300$ K, $T_s = 31.25$ ns, $\eta = 0.4$, and $I_s = 3.9 \times 10^{-10}$ nA.

IV. Numerical Results

In order to generate a sample function of the spatial distribution of the signal incident upon the detector plane, sample fields were generated using a Kolmogorov phase-screen program [9] with an atmospheric correlation length of $r_0 = 4$ cm, representing moderate turbulence, resulting in a matrix of complex signal amplitudes. The field intensity generated in the detector plane by the simulation then was integrated over the elements of a $16 \times 16 = 256$ detector array that was dimensioned to encompass the significant extent of the signal distribution in the detector plane, corresponding roughly to an optimized single-detector design. A constant average background photon energy of $\bar{n}_b$ is assumed over each detector element. For a given sample function of the intensity distribution, the 256 detector elements were sorted in decreasing order of average signal energy, and M-ary PPM symbol-error probabilities were calculated for increasing numbers of detectors, starting with the detector with the highest incident signal energy [1], in order to specify the adaptive synthesized detector. Note that the results presented here are for a single realization of the turbulent signal distribution. However, in [1] it was observed that different turbulence realizations (with the same atmospheric correlation-length parameter value) did not result in significantly different array detection results for the photon-counting channel. Because the photon arrival process is the same for both models, it is reasonable to assume that this will hold for the APD detector array as well.

Performance results were obtained for two types of receivers: (1) the adaptive synthesized detector (the optimum number of unweighted detector elements are used) and (2) the single large detector (all 256 detector elements are given unity weight, effectively synthesizing a nonadaptive single large detector). The results of the APD array simulations are shown in Figs. 2 through 9 and are compared with analogous

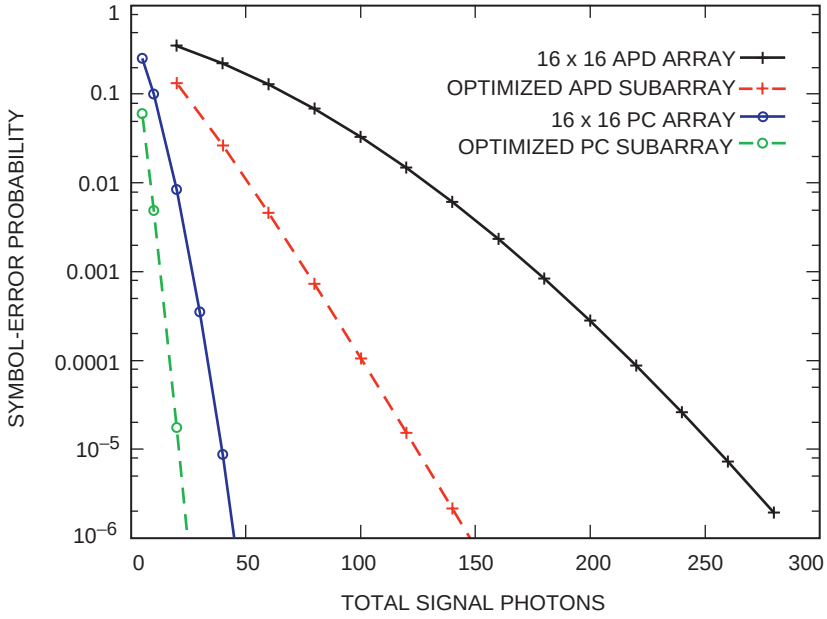

Fig. 2. PPM symbol-error probabilities for 2-PPM, $\bar{n}_b = 0.1$ absorbed background photon per detector element per slot.

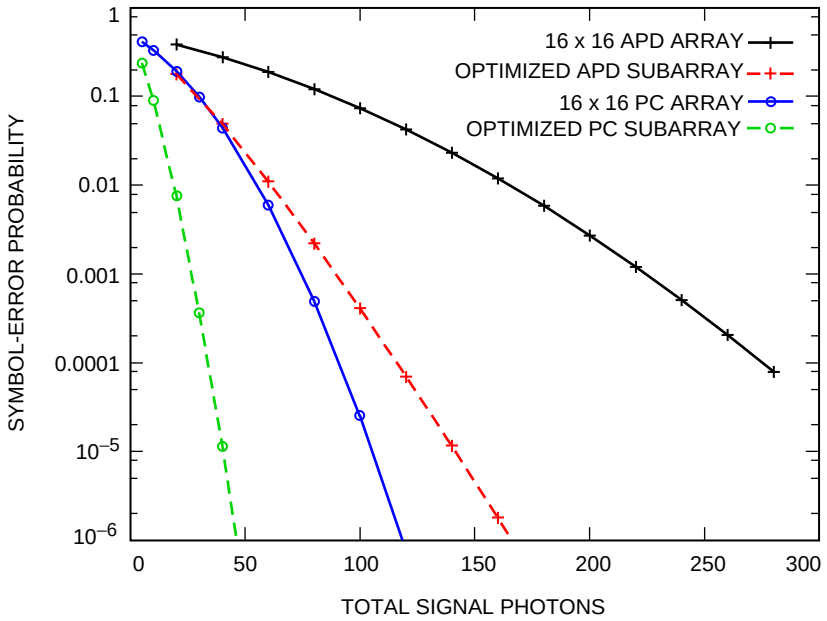

Fig. 3. PPM symbol-error probabilities for 2-PPM, $\bar{n}_b = 1.0$ absorbed background photon per detector element per slot.

photon-counting detector results. The APD results were obtained using a Gaussian approximation for the distribution of the detector output, composed of Webb-distributed secondary electrons plus additive Gaussian noise. The photon-counting results assumed Poisson-distributed observables, which accurately represent the statistics of multimode signal plus background radiation under typical operating conditions [8]. PPM modulation with $M = 2$, 4, 16, and 256 was investigated, operating in the presence of low-to-

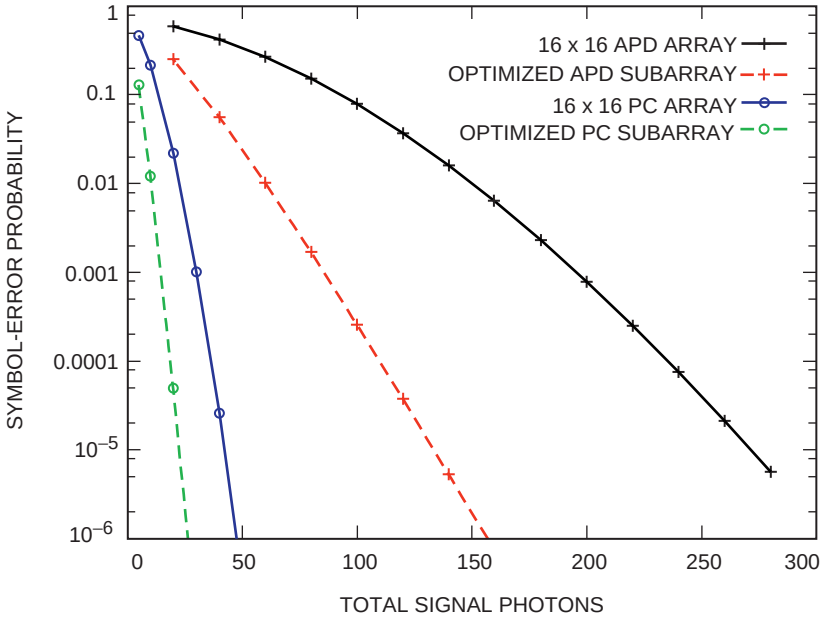

Fig. 4. PPM symbol-error probabilities for 4-PPM, $\bar{n}_b = 0.1$ absorbed background photon per detector element per slot.

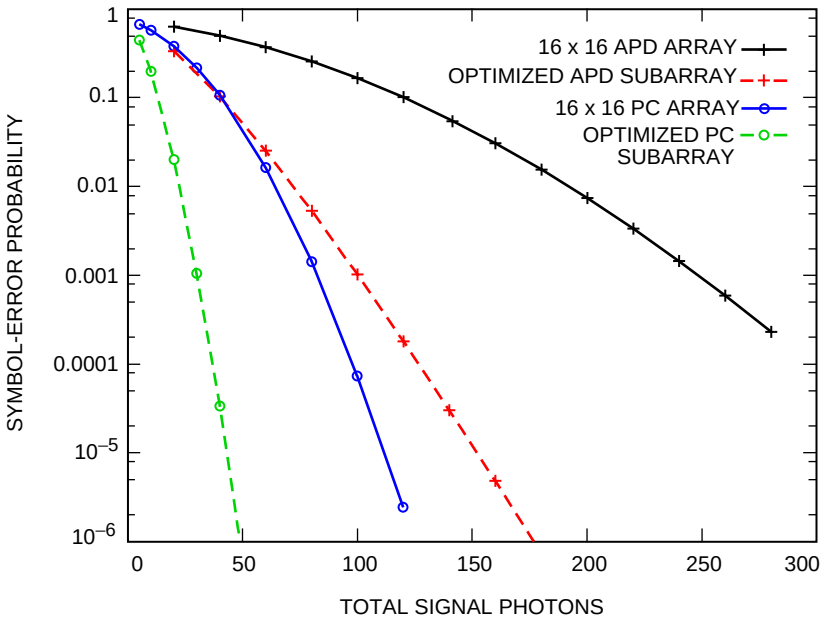

Fig. 5. PPM symbol-error probabilities for 4-PPM, $\bar{n}_b = 1.0$ absorbed background photon per detector element per slot.

moderate background levels that generate an average of 0.1 absorbed photon per detector element over each slot time (or an average of 25.6 absorbed photons per slot over the entire array, which can also be viewed as a single large detector), as well as high background levels of 1 absorbed photon per detector element per slot (or 256 absorbed photons per slot over the entire array). For the 256-PPM photon-counting results shown in Figs. 8 and 9, accurate computation of the exact symbol probability was prohibitively complicated, so a union bound (as discussed in [1]) was used.

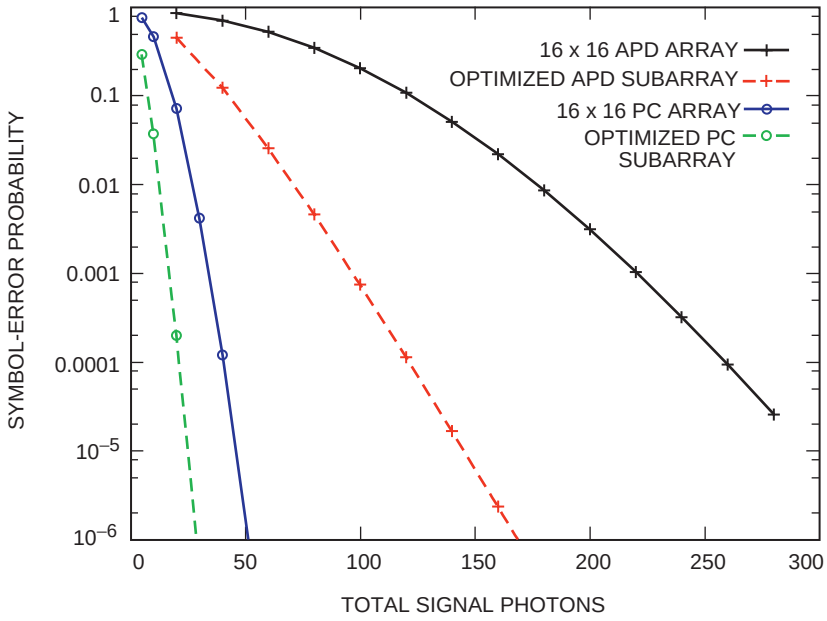

Fig. 6. PPM symbol-error probabilities for 16-PPM, $\bar{n}_b = 0.1$ absorbed background photon per detector element per slot.

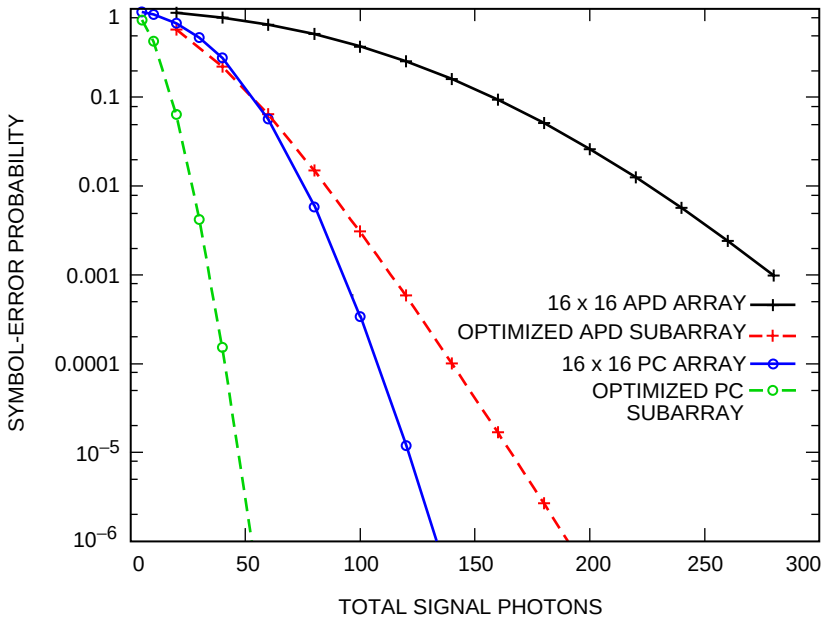

Fig. 7. PPM symbol-error probabilities for 16-PPM, $\bar{n}_b = 1.0$ absorbed background photon per detector element per slot.

The results for low-to-moderate background levels (0.1 absorbed photon per detector element per slot) are shown in Figs. 2, 4, 6, and 8 for each value of M. The gain from APD array processing over a single APD is about 3.6 dB at a symbol-error probability of 0.001 for all values of M. It is apparent that for the case of low-to-moderate background levels further improvements are possible with the use of an adaptive APD array to reduce the size of the subarray, thus limiting the background contribution to the total noise process.

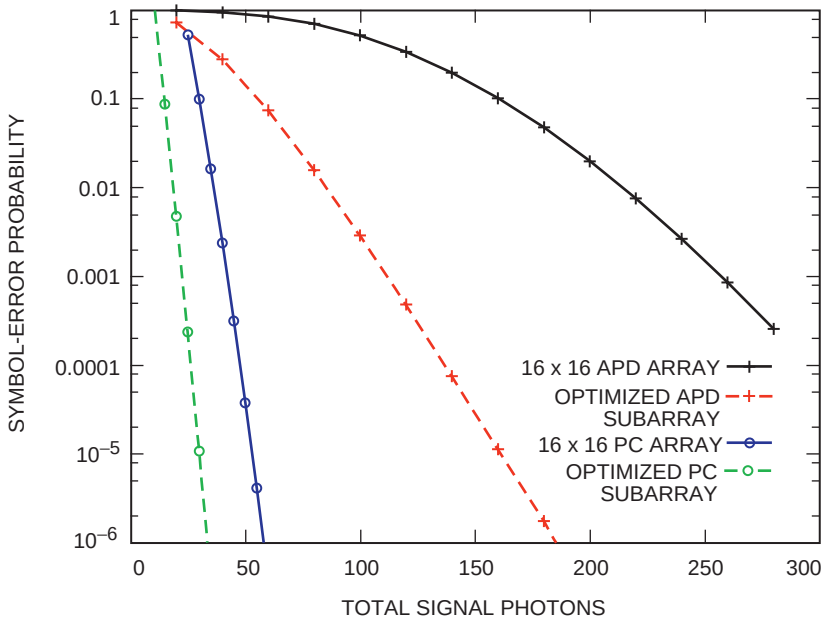

Fig. 8. PPM symbol-error probabilities for 256-PPM, $\bar{n}_b = 0.1$ absorbed background photon per detector element per slot.

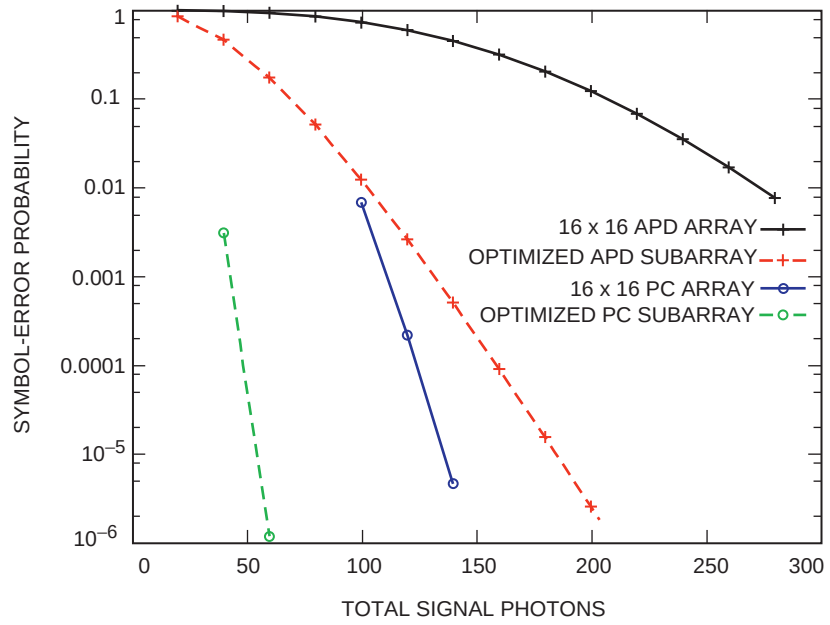

Fig. 9. PPM symbol-error probabilities for 256-PPM, $\bar{n}_b = 1.0$ absorbed background photon per detector element per slot.

When operating in high background environments characterized by an average of 1 absorbed photon per detector element per slot (or 256 absorbed photons for the entire array, or for a single large detector), the improvements due to APD array processing tend to be greater. At a symbol-error probability of 0.001, adaptive APD array processing now yields approximately 4 dB over the single large APD for all cases considered. The reason is that the background contribution to the total noise variance in Eq. (5)

dominates; reducing the sum of the elemental background contributions by restricting the observation region to a much smaller subarray therefore results in a proportionally smaller noise variance.

While significant, the improvements demonstrated by the use of adaptive APD arrays over a single large APD detector are nevertheless smaller than gains achievable through the use of adaptive photon-counting detector arrays [1], as shown in Figs. 2 through 9. The reason is that photon-counting detectors are not hampered by excess noise due to the avalanche multiplication process or by thermally generated circuit noise, which tend to limit the performance of conventional APD detectors. For the case of low-to-moderate background levels, the use of adaptive photon-counting arrays results in gains of 7 dB to 7.5 dB over the APD array, or 10.6 dB to 11.1 dB over the single large APD, at symbol-error probabilities of 0.001. For the high background case, the corresponding improvements are 5 dB to 5.5 dB over the APD array and 9 dB to 9.5 dB over the single large APD. Adaptive photon-counting arrays therefore provide greatly enhanced capabilities for the reception of PPM-modulated optical signals through the terrestrial atmosphere.

V. Summary and Conclusions

The results of earlier studies concerning the use of optical focal-plane photon-counting detector arrays together with adaptive signal processing to combat the effects of atmospheric turbulence [1] have been extended to include APD arrays used in a similar configuration. The total detector output process, composed of APD secondary electrons due to absorbed photons together with additive circuit noise of thermal origin, was modeled as a Gaussian random process with mean and variance consistent with the statistics of the component processes. Adaptive array performance was evaluated for operation in both low and high background environments for the case of PPM-modulated received fields, and compared with the performance of the photon-counting adaptive array previously documented in [1]. It was found that while adaptive APD detector arrays provided improvements of 3.6 dB to 4 dB over the performance of single large APD detectors designed to collect most of the received signal, the use of photon-counting arrays instead of single large APD detectors provided much greater additional improvements, amounting to as much as 11 dB in low-to-moderate background environments and up to 9.5 dB in high background environments. Improvements of this magnitude warrant serious consideration of the adaptive photon-counting array technology for future DSN optical communications applications.

References

[1] V. Vilnrotter and M. Srinivasan, "Adaptive Detector Arrays for Optical Communications Receivers," *The Telecommunications and Mission Operations Progress Report 42-141, January–March 2000*, Jet Propulsion Laboratory, Pasadena, California, pp. 1–22, May 15, 2000.
http://tmo.jpl.nasa.gov/tmo/progress_report/42-141/141H.pdf

[2] F. M. Davidson and X. Sun, "Gaussian Approximation Versus Nearly Exact Performance Analysis of Optical Communications Systems with PPM Signaling and APD Receivers," *IEEE Transactions on Communications*, vol. COM-36, pp. 1185–1192, November 1988.

[3] R. J. McIntyre, "The Distribution of Gains in Uniformly Multiplying Avalanche Photodiodes: Theory," *IEEE Transactions on Electron Devices*, vol. ED-19, pp. 703–713, June 1972.

[4] P. P. Webb, R. J. McIntyre, and J. Conradi, "Properties of Avalanche Photodiodes," *RCA Review*, vol. 35, pp. 234–278, June 1974.

[5] M. Srinivasan and V. Vilnrotter, "Symbol-Error Probabilities for Pulse-Position Modulation Signaling With an Avalanche Photodiode Receiver and Gaussian Thermal Noise," *The Telecommunications and Mission Operations Progress Report 42-134, April–June 1998*, Jet Propulsion Laboratory, Pasadena, California, pp. 1–11, August 15, 1998.
http://tmo.jpl.nasa.gov/tmo/progress_report/42-134/134E.pdf

[6] V. Vilnrotter, M. Simon, and M. Srinivasan, "Maximum Likelihood Detection of PPM Signals Governed by an Arbitrary Point Process Plus Additive Gaussian Noise," *Electronics Letters*, vol. 35, pp. 1132–1133, July 1999.

[7] R. M. Gagliardi and S. Karp, *Optical Communications*, New York: John Wiley and Sons, Inc., 1995.

[8] E. V. Hoversten, R. O. Harger, and S. J. Halme, "Communications Theory for the Turbulent Atmosphere," *Proceedings of the IEEE*, pp. 1626–1650, October 1970.

[9] P. Negrete-Regagnon, "Practical Aspects of Image Recovery by Means of the Bispectrum," *Journal of the Optical Society of America*, vol. 13, pp. 1557–1576, July 1996.

[10] M. Jeganathan and S. Mecherle, *FOCAS 2.0: Free-Space Optical Communications Analysis Software*, Jet Propulsion Laboratory, Pasadena, California, May 1998.